THE JOURNAL OF PHYSICAL CHEMISTRY C

ARTICLE

pubs.acs.org/JPCC

Elastic, Electronic, and Optical Properties of Two-Dimensional Graphyne Sheet

Jun Kang,[†] Jingbo Li,[*,†,‡] Fengmin Wu,[‡] Shu-Shen Li,[†] and Jian-Bai Xia[†]

[†]State Key Laboratory for Superlattices and Microstructures, Institute of Semiconductors, Chinese Academy of Sciences, P.O. Box 912, Beijing 100083, China

[‡]Zhejiang Normal University, Jinhua 321004, Zhejiang Province, China

ABSTRACT: The elastic, electronic, and optical properties of the 2D graphyne sheet, which consists of hexagonal carbon rings and acetylenic linkages, are investigated from first-principles calculations. Graphyne has a Poisson's ratio of 0.417 and an in-plane stiffness of 10.36 eV/Å^2. Compared with graphene, graphyne is much softer because of its relatively smaller number of bonds. The band structure of graphyne is calculated using both generalized gradient approximation and hybrid functional, and the band gap predicted by the latter is twice as much as that given by the former. It is also shown that the energy bands of graphyne can be divided into several regions according to bonding character. The optical property of graphyne is found to be strongly anisotropic. For electric field parallel to the graphyne plane, strong optical adsorption is observed in low-energy region, whereas for the electric field perpendicular to the graphyne plane, the adsorption in the low-energy region is very weak. What's more, the response of the band gap of graphyne to uniform strain is also studied, and we show that the band gap can be continuously modified under the strain.

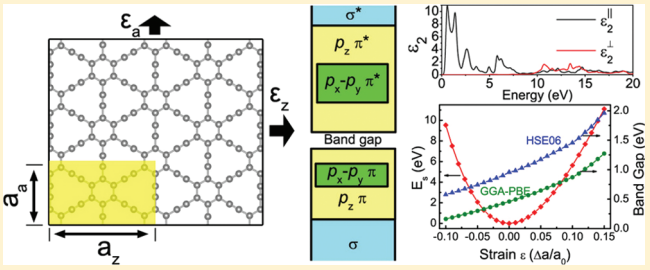

INTRODUCTION

The allotrope of carbon has long been a topic of interest.[1,2] There are two natural carbon allotropes, namely, diamond and graphite, which contain sp^3 and sp^2 hybridized carbon atoms, respectively. Since the 1980s, many new carbon allotropes, such as fullerenes,[3] carbon nanotubes,[4] and graphene[5] have been successfully synthesized. Graphyne, predicted by Baughman et al.,[6] is a new form of carbon that consists of planar carbon sheets containing sp and sp^2 carbon atoms. In 2D graphyne sheet, hexagonal carbon rings are joined together by acetylenic linkages, forming so-called phenylacetylene (PA) structure,[7] and it has the same symmetry as graphene. Because of high π-conjunction, PA structures have interesting properties, and there are many studies focused on PA-based systems. For instance, molecules consisting of PA units exhibit strong negative differential resistance[8] and are good candidates for molecular memory devices.[9−11] Tada et al. have explained the directional energy flow of the nanostar dendrimer through molecular orbital analysis.[12] The band structures and frontier crystal orbitals of a series of PA-based chains and sheets have been investigated by Kondo et al.[7] In graphyne, the presence of acetylenic linkage introduces nonzero band gap in graphyne sheet,[7,13] which is absent in graphene. Although the synthesization of graphyne has not been reported, approaches to fabricate its substructures have been developed.[14−16] More recently, Li et al. have successfully generated large area films of graphdiyne, which belongs to the same family as graphyne, on copper surface by a cross-coupling reaction using hexaethynylbenzene.[17] Through an anodic aluminum oxide template catalyzed by Cu foil, they have also prepared graphdiyne nanotube arrays.[18] These exciting experimental progresses suggest that the synthesization of graphyne is hopeful and stimulate many theoretical researches on the properties, such as band gap,[19,20] charge mobility,[21] and lithium storage capacity,[22] of graphyne and its related structures.

Although much knowledge has been gained about graphyne, many questions are still worth discussing. For example, (i) The elastic property of graphyne has not been examined yet. Is it stiffer or softer than graphene? (ii) In previous first-principles studies, the band structure of graphyne is calculated using local density approximation (LDA) or generalized gradient approximation (GGA),[13,19] which causes underestimation of band gap. To describe the band structure of graphyne better, methods going beyond LDA and GGA are needed, such as hybrid functionals. (iii) The optical property of graphyne is still unclear. Because of its 2D feature, graphyne sheet may possesses anisotropic optical property, which is similar as boron nitride sheet.[23] (iv) Numerous investigations have demonstrated that the properties of low-dimensional material can be modified by strain.[24−27] It would be interesting to see the effect of strain on the electronic property of graphyne.

In this work, we investigate the elastic, electronic, and optical properties of 2D graphyne sheet from first-principles calculations. We calculate the elastic parameters of graphyne and compare

Received: July 15, 2011
Revised: September 10, 2011
Published: September 13, 2011

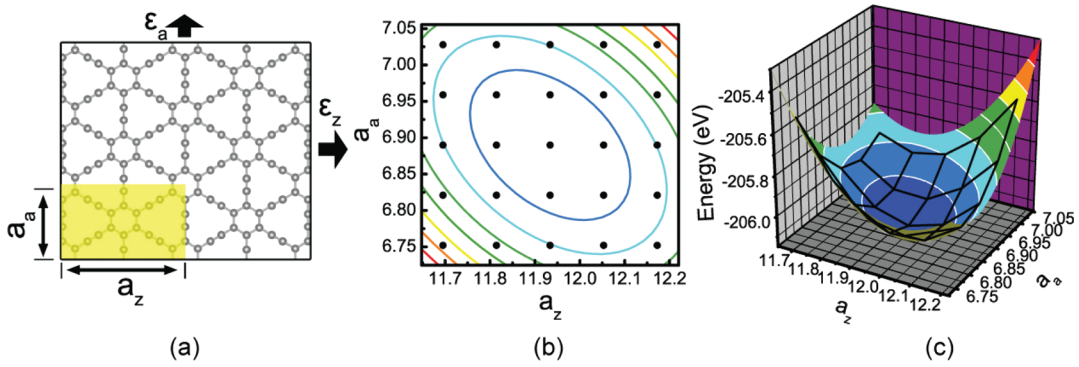

Figure 1. (a) Geometry structure of graphyne. The rectangular supercell used to calculate the elastic properties is indicated by shadow. a_a and a_z are the lattice constants along armchair and zigzag directions, respectively. Strain is applied by varying a_z and a_a. (b) Mesh grid used for total energy calculations. a_z and a_a are given in angstroms. (c) 3D plot of energy surface of graphyne. The dark grid is the calculated result, and the colored surface is the fitted value.

its stiffness with that of graphene. Band structure of graphyne is discussed, and we present both GGA and hybrid functional calculated results. The optical property of graphyne is also studied, and strong anisotropy is observed. Furthermore, we show that the band gap of graphyne can be tuned continuously under uniform strain.

COMPUTATIONAL METHODS

The calculations are performed using the frozen-core projector-augmented wave method[28,29] as implemented in the Vienna ab initio simulation package (VASP).[30,31] The generalized gradient approximation of Perdew−Burke−Ernzerhof (GGA-PBE)[32] is adopted for exchange-correlation functional. Because GGA underestimated the band gap, the Heyd−Scuseria−Ernzerhof (HSE06)[33,34] hybrid functional is also used for band structure calculation. Energy cutoff for plane-wave expansion is set to 400 eV. Brillouin zone sampling is performed with Monkhorst-Pack (MP) special k-point meshes[35] including Γ-point. For rectangle unit cell, a 7 × 11 × 1 k-grid is chosen, whereas for hexagonal unit cell, a 11 × 11 × 1 k-grid is used. To obtain smooth optical spectra, the k-grid is increased to 31 × 31 × 1 in optical property calculation. A vacuum layer of 11 Å is added along the z direction to avoid interaction between adjacent graphyne layers. Structure relaxation is stopped when the Hellmann−Feynman force on each atom is <0.02 eV/Å. The calculations of band alignment are based on the branching point energy (BPE),[36−39] which is defined as the weighted average of eigenenergies over the MP meshes.[40] The lowest conduction band and the highest valence band are included for calculation.

RESULTS AND DISCUSSION

Elastic Properties. The geometry structure of monolayer graphyne is shown in Figure 1a. In graphyne, sp^2 hybridized C atoms form hexagonal rings, and they are joined together by sp hybridized acetylenic linkages. The optimized lattice constant a_0 is 6.89 Å, in good agreement with other calculations.[13,19,22]

Because of its hexagonal symmetry, the elastic properties of graphyne is isotropic and can be described by two independent constants: Young's modulus Y and Poisson's ratio ν. Young's modulus can be defined as the second derivative of the total energy with respect to the strain at the equilibrium volume, given as $Y = (1/\Omega_0)(\partial^2 E/\partial\varepsilon^2)$, where Ω_0 is the equilibrium volume, E is the total energy, and ε is uniaxial strain. However, because of its 2D character, the thickness h of graphyne cannot be directly defined. Therefore, there are uncertainties when calculating equilibrium volume as well as Young's modulus. To avoid the uncertainties, one can calculate the in-plane stiffness instead of Young's modulus. The in-plane stiffness C is given by $C = (1/S_0)(\partial^2 E/\partial\varepsilon^2)$, where S_0 is the equilibrium area. The other parameter, Poisson's ratio ν, is the ratio of the transverse strain to the axial strain, namely, $\nu = -\varepsilon_{trans}/\varepsilon_{axial}$. To calculate the elastic properties of graphyne, we use the method described in ref 24. First, we construct a rectangular unit cell of graphyne that contains 24 C atoms, as seen in Figure 1a. One of the lattice vectors of the rectangular cell is along the zigzag direction (the (n, n) direction in hexagonal cell), and the other is along the armchair direction (the (n,0) direction in hexagonal cell). The two lattice constants are a_z = 11.93 Å and a_a = 6.89 Å, respectively. By changing the lattice constants, strain is applied to the unit cell in the range from −0.02 to 0.02 for each direction, with an increment of 0.01. We obtained 25 data points, as presented in Figure 1b. At each point, the atomic positions are relaxed, and the total energy of the unit cell is calculated. The dark grid in Figure 1c shows the calculated results. The results are then fitted by the formula $E = c_1\varepsilon_z^2 + c_1\varepsilon_a^2 + c_2\varepsilon_z\varepsilon_a + E_0$, in which E_0 is the total energy at equilibrium state, and ε_z and ε_a are the strain along zigzag and armchair directions, respectively. Using this formula, the Poisson's ratio and in-plane stiffness can be determined. Assume that the stress is along the armchair direction and the corresponding transverse and axial strains are $\Delta\varepsilon_z$ and $\Delta\varepsilon_a$. From $\partial E/\partial\Delta\varepsilon_z = 0$, one obtains $\Delta\varepsilon_z = -(c_2/2c_1)\Delta\varepsilon_a$, and the Poisson's ratio ν is $c_2/2c_1$. The total energy can be written as $E = c_1\nu^2(\Delta\varepsilon_a)^2 + c_1(\Delta\varepsilon_a)^2 + c_2\nu(\Delta\varepsilon_a)^2 + E_0$. Then, the in-plane stiffness can be calculated by $C = (1/S_0)(2c_1\nu^2 + 2c_1 + 2c_2\nu) = (1/S_0)(2c_1 - c_2^2/2c_1)$. The fitted formula is $E = 515.86\varepsilon_z^2 + 515.86\varepsilon_a^2 + 430.46\varepsilon_z\varepsilon_a + E_0$ (the unit of energy is electronvolts), and the 3D energy-strain plot is shown in Figure 1c. Hence the Poisson's ratio of graphyne is 0.417, and its in-plane stiffness is 10.36 eV/Å^2 or 166 N/m. Experimentally, it is reported that the in-plane stiffness of graphene is 340 ± 50 N/m,[41] which is twice larger than that of graphyne. In view of the in-plane stiffness, graphyne is much softer than graphene. This can be understood by the different number of bonds in graphene and graphyne. In graphene, each C atom is three-fold coordinated, whereas in graphyne the average coordination number of

C atom is 2.5. The number of bonds in graphyne is fewer than that of graphene, leading to the relatively smaller in-plane stiffness.

Band Structure. The band structure of graphyne has been calculated by Narita et al. on the DFT-LDA level.[13] They concluded that graphyne has a direct band gap of 0.52 eV at the M point in the hexagonal Brillouin zone. They also showed that the effective masses of carriers in graphyne are anisotropic. The effective masses along the M−K direction are much smaller than those along M−Γ direction. Here we calculate the band structure of graphyne using GGA-PBE first, as shown by the lines in Figure 2a. We get very similar band structure as in ref 13. The band gap is found to be 0.46 eV, which is consistent with other GGA-PBE calculation.[19] The effective masses are also calculated using $m^* = \hbar^2/(\partial^2 E/\partial k^2)$, and we choose the k points very close to M point (within 0.04 Å^{-1}). The results are listed in Table 1. Compared with ref 13, the calculated effective masses here are slightly larger, but the trend is still the same; that is, the m^* values along the M−Γ direction are two times more than those along the M−K direction. However, it is well known that the band gap of semiconductor is underestimated by LDA and GGA. In contrast, hybrid functionals such as HSE06 can reproduce the experimentally measured band gap quite well and give excellent description of the electronic structure of semiconductor.[42] In our test calculations, the band gap of diamond predicated by GGA-PBE is 4.11 eV, whereas it is 5.28 eV predicted by HSE06. The latter is in good agreement with an experimental value of 5.47 eV.[43] The HSE06 calculated band structure of graphyne is presented in Figure 2a by open circles. A 0.96 eV band gap is obtained, which is twice as much as GGA-PBE value. The HSE06 calculated effective masses are also listed in Table 1. Compared with GGA-PBE results, HSE06 gives larger m^* along the M−K direction and slightly smaller m^* along M−Γ. Except for the band gap, the band structures given by GGA-PBE and HSE06 exhibit similar features. Therefore we expect that there are no obvious differences between the electronic properties calculated by these two functionals, and all of the following results are obtained using GGA-PBE if not specified.

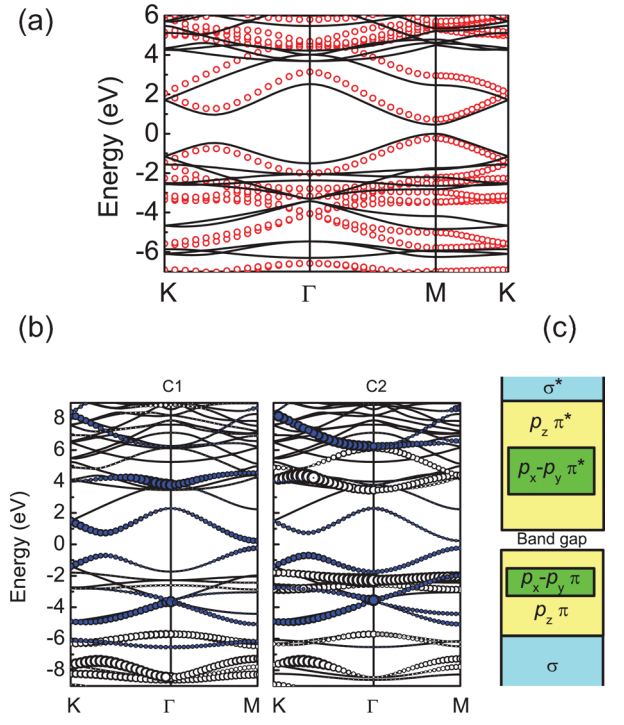

Figure 2. (a) Band structure of graphyne. Solid lines and open circles are GGA-PBE and HSE06 calculated results, respectively. The bands are aligned according to BPE and the energy of VBM calculated by GGA-PBE is set to zero. (b) Projected band structures for two C atoms with sp^2 hybridization (C1) and sp hybridization (C2) in graphyne. Contributions from p_x and p_y orbitals are represented by open circles, and the contributions from p_z orbital are indicated by solid circles. (c) Division of energy region according to different bonding types.

As mentioned above, there are both sp^2 and sp hybridized C atoms in graphyne, resulting in several different bond types. The bond between two sp^2 C atoms has $\sigma + \pi$ character. The σ bond is contributed by $p_x + p_y$ and s orbitals of C atom, and the π bond comes from the p_z orbital. Two sp C atoms are $\sigma + 2\pi$ bonded. The characters of the σ bond and one of the π bonds are the same as sp^2−sp^2 bonding, whereas the other π bond is contributed by $p_x + p_y$ orbitals, which is absent in sp^2−sp^2 bonding. The bond between C-sp^2 and C-sp is single σ bond and has $p_x + p_y$ and s characters. In Figure 2b, the projection of atomic orbitals on the energy band is plotted for two C atoms, C1 and C2. C1 is on the hexagonal ring with sp^2 hybridization, and C2 is on the acetylenic linkage with sp hybridization. On the basis of the projected band structure, the band structure of graphyne can be divided into several energy regions according to the bonding character, as seen in Figure 2c. The valence bands correspond to bonding states. In the region below −6 eV, the bands are dominated by p_x and p_y states of both C atoms, and they can be classified as bonding σ bands. The bonding p_z π bands range from −6 eV to VBM because the p_z states of both C atoms have significant contributions in this region. Besides, it is notable that several bands with p_x and p_y characters can be found between −3 and −2 eV. These p_x and p_y states mainly come from C2 and the contribution of C1 is neglectable. Therefore, we can conclude that these bands are bonding p_x−p_y π bands, which come from the bonding between two sp C atoms. The conduction bands correspond to antibonding states. The antibonding p_z π^* bands range from CBM to ∼11 eV. The antibonding p_x−p_y π^* bands appear between 4 and 6 eV. In addition, the antibonding σ^* bands are found above 9 eV. The p_z π and p_z π^* bands are much wider than p_x−p_y π and p_x−p_y π^* bands, indicating that the p_z π bond is much more delocalized than p_x−p_y π bond. This can be easily understood because both sp^2 and sp C atoms have p_z π bonds and there are large overlaps between p_z orbitals of adjacent C atoms. Nevertheless, p_x−p_y π bonds exist only in sp C atoms.

Table 1. Band Gap E_g and Effective Masses for Electrons (m_c^*) and Holes (m_v^*) of Graphyne[a]

	E_g (eV)	m_c^*/m_0 (M−Γ)	m_c^*/m_0 (M-K)	m_v^*/m_0 (M-Γ)	m_v^*/m_0 (M−K)
GGA-PBE	0.46	0.20	0.080	0.21	0.083
HSE06	0.96	0.18	0.11	0.19	0.12
ref 13	0.52	0.15	0.063	0.17	0.066

[a] Values obtained by both GGA-PBE and HSE06 are presented. The results of Narita et al.[13] are also listed for comparison.

They are separated spatially by the hexagonal rings, leading to small overlaps.

Optical Properties. To investigate the optical properties of graphyne, we have calculated the imaginary part of the dielectric function, as displayed in Figure 3. Both GGA-PBE and HSE06 give similar spectra except for an energy shift, so only GGA-PBE results is plotted. Strong anisotropy in the optical spectra is observed, especially in the low-energy region. If the electric field is parallel to the graphyne plane (in-plane polarization), then there is strong optical adsorption in the range of 0 to 8 eV. If the electric field is perpendicular to the graphyne plane (out of plane polarization), then the imaginary part of the dielectric function is less than 0.01 below 9 eV, indicating neglectable optical adsorption in this region.

On the basis of symmetry arguments and the division of band structure in Figure 2, the dominant optical transitions in different energy region of the optical spectrum can be roughly determined. With respective to the graphyne plane, the σ and σ^* states, as well as the p_x-p_y π and p_x-p_y π^* states, have even parity, while p_z π and p_z π^* states have odd parity. Under in-plane and out-of-plane polarization, the transitions are allowed between states with the same and different parity, respectively. Therefore, for in-plane polarization, the adsorption from 0 to 5 eV comes from the p_z $\pi \rightarrow p_z$ π^* transition. Between 6 and 8 eV, the p_x-p_y $\pi \rightarrow p_x-p_y$ π^* transition dominates. In the range of 10 to 14 eV, the adsorption can be attributed to the p_x-p_y $\pi \rightarrow \sigma^*$ and $\sigma \rightarrow p_x-p_y$ π^* transitions. The adsorption over 14 eV results from $\sigma \rightarrow \sigma^*$ transitions. For out-of-plane polarization, the weak adsorption below 9 eV is contributed by p_x-p_y $\pi \rightarrow p_z$ π^* and p_z $\pi \rightarrow p_x-p_y$ π^* transitions, whereas over 9 eV the adsorption mainly originates from $\sigma \rightarrow p_z$ π^* and p_z $\pi \rightarrow \sigma^*$ transitions.

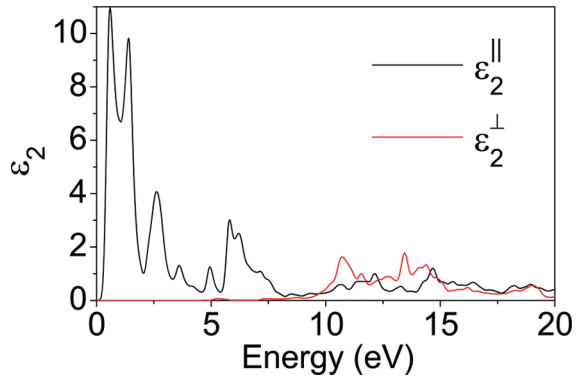

Figure 3. Calculated imaginary part of the dielectric function of graphyne. Results for electric field parallel to the graphyne plane ($\varepsilon_2^{\parallel}$) and perpendicular to the graphyne plane ($\varepsilon_2^{\perp}$) are given.

Tunable Band Gap under Uniform Strain. Finally we discuss the behavior of graphyne under uniform strain. Computations are carried out using hexagonal private cell. The lattice constant a is varied with the strain value from −0.10 to 0.15 in step of 0.01. At each point the strain energy (energy difference between strained and equilibrium systems) and band gap are calculated. The results are shown in Figure 4a. For both tensile and compressive strain, within the imposed strain range, the strain energy increases monotonously as strain increases, demonstrating the deformation of graphyne is elastic. Once the stress is removed, graphyne can go back to its equilibrium state. We have also calculated the derivative of strain energy with respect to strain. It is found that the harmonic approximation is well applied with $-0.02 < \varepsilon < 0.02$. Beyond this value the E_s-ε curve becomes inharmonic because the contributions of higher order terms are larger than 10% and noticeable.

The band gaps are calculated by both GGA-PBE and HSE06, and they give the same trend. For $-0.10 < \varepsilon < 0.15$, the direct gap character of graphyne is maintained, and it exhibits tunable band gap under strain. In the case of tensile strain, the gap value increases as strain increases, whereas it decreases under compressive strain. At $\varepsilon = 0.15$, the band gap is ∼1 eV larger than that in equilibrium state, whereas it is ∼0.3 eV lower at $\varepsilon = -0.10$. Under tensile strain, in the strain range from 0 to 0.10, the increasing of band gap is almost linear. The calculated slopes using GGA-PBE and HSE06 are 4.15 and 5.13 eV, respectively. When ε exceeds 0.10, the linear E_g versus ε relationship is still observed, but the slopes are nearly doubled and become 8.10 (GGA-PBE) and 10.14 eV (HSE06). Under compressive strain, the band gap also decreases linearly with increasing strain value, and the slopes are 2.97 (GGA-PBE) and 3.71 eV (HSE06). We suppose the variation of band gap is related to the change in the width of p_z π and p_z π^* bands. When tensile strain is applied to graphyne, the distance between C atoms increases and the overlap of p_z states between C atoms decreases, narrowing the width of p_z π and p_z π^* bands. As a result, the VBM moves downward, the CBM moves upward, and the band gap increases. When compressive strain is applied, the overlap between p_z states increases, so the bandwidth becomes wider. Therefore the VBM moves upward, the CBM moves downward, the band gap decreases. Figure 4 b presents the band structure of graphyne

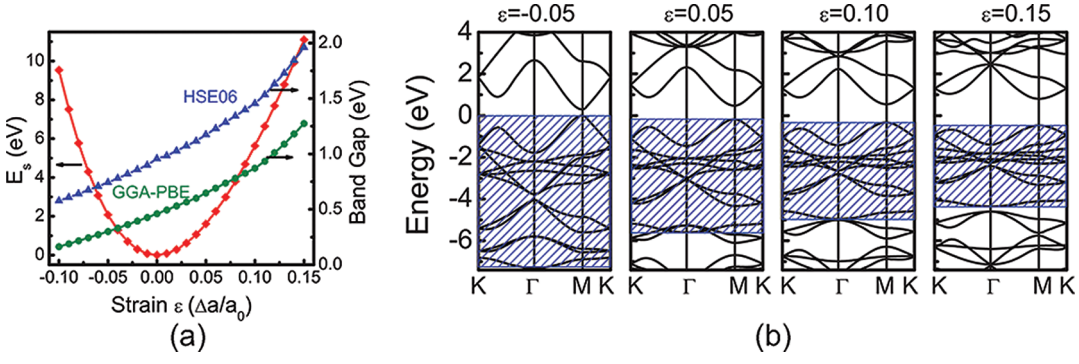

Figure 4. (a) Variation of strain energy and band gap of graphyne under uniform strain. The band gaps are calculated using both GGA-PBE (green circles) and HSE06 (blue triangles). (b) Band structure of graphyne under different strain values. The shaded regions indicate the p_z π bands. The band structures are aligned using the BPE. The energy of the VBM for $\varepsilon = -0.05$ is set as zero.

under different strain values, and the p_z π bands are shown by shade. It can be seen the width of p_z π band decreases (increases) obviously under tensile (compressive) strain, confirming the prospection. The movement of CBM or VBM also agrees with our anticipation. The tunable band gap of graphyne under uniform strain promises its applications in nanomechanics.

CONCLUSIONS

In summary, we have carried out a first-principles study on the elastic, electronic, and optical properties of 2D graphyne sheet. The Poisson's ratio of graphyne is 0.417, and its in-plane stiffness is 10.36 eV/Å^2. Compared with graphene, graphyne is much softer because of its lower coordination number. The band structure of graphyne is calculated by both GGA-PBE and HSE06. HSE06 predicts a 0.96 eV band gap, which is twice as much as GGA-PBE gives. Different bonding types in graphyne are discussed, and it is demonstrated that the energy bands of graphyne can be divided into several regions according to bonding character. The optical spectra of graphyne exhibit strong anisotropy. In the low-energy region, the optical adsorption is significant for in-plane polarization but neglectable for out of plane polarization. On the basis of symmetry arguments and the division of band structure, the dominant optical transitions in different energy region is also analyzed. Finally, we show that the band gap of graphyne can be modified continuously under uniform strain. What's more, this behavior can be understood by means of bandwidth variation. We believe these findings will be helpful for the application of graphyne in the future.

AUTHOR INFORMATION

Corresponding Author
*E-mail: jbli@semi.ac.cn.

ACKNOWLEDGMENT

J.L. gratefully acknowledges financial support from the "Hundred Talents Program" of the Chinese Academy of Science and National Science Fund for Distinguished Young Scholar (grant no. 60925016). We acknowledge the computing resources provided by Supercomputing Center, CNIC, CAS.

REFERENCES

(1) Diederich, F.; Kivala, M. *Adv. Mater.* **2010**, *22*, 803–812.
(2) Hirsch, A. *Nat. Mater.* **2010**, *9*, 868–871.
(3) Kroto, H.; Heath, J.; O'Brien, S.; Curl, R.; Smalley, R. *Nature (London)* **1985**, *318*, 162–163.
(4) Iijima, S. *Nature (London)* **1991**, *354*, 56–58.
(5) Novoselov, K. S.; Geim, A. K.; Morozov, S. V.; Jiang, D.; Zhang, Y.; Dubonos, S. V.; Grigorieva, I. V.; Firsov, A. A. *Science* **2004**, *306*, 666.
(6) Baughman, R. H.; Eckhardt, H.; Kertesz, M. *J. Chem. Phys.* **1987**, *87*, 6687–6699.
(7) Kondo, M.; Nozaki, D.; Tachibana, M.; Yumura, T.; Yoshizawa, K. *Chem. Phys.* **2005**, *312*, 289–297.
(8) Chen, J.; Reed, M. A.; Rawlett, A. M.; Tour, J. M. *Science* **1999**, *286*, 1550–1552.
(9) Seminario, J. M.; Zacarias, A. G.; Derosa, P. A. *J. Phys. Chem. A* **2001**, *105*, 791–795.
(10) Seminario, J. M.; Zacarias, A. G.; Derosa, P. A. *J. Chem. Phys.* **2002**, *116*, 1671–1683.
(11) Taylor, J.; Brandbyge, M.; Stokbro, K. *Phys. Rev. B* **2003**, *68*, 121101.
(12) Tada, T.; Nozaki, D.; Kondo, M.; Yoshizawa, K. *J. Phys. Chem. B* **2003**, *107*, 14204–14210.
(13) Narita, N.; Nagai, S.; Suzuki, S.; Nakao, K. *Phys. Rev. B* **1998**, *58*, 11009–11014.
(14) Kehoe, J. M.; Kiley, J. H.; English, J. J.; Johnson, C. A.; Petersen, R. C.; Haley, M. M. *Org. Lett.* **2000**, *2*, 969–972.
(15) Haley, M. M. *Pure Appl. Chem.* **2008**, *80*, 519–532.
(16) Yoshimura, T.; Inaba, A.; Sonoda, M.; Tahara, K.; Tobe, Y.; Williams, R. V. *Org. Lett.* **2006**, *8*, 2933–2936.
(17) Li, G.; Li, Y.; Liu, H.; Guo, Y.; Li, Y.; Zhu, D. *Chem. Commun.* **2010**, *46*, 3256–3258.
(18) Li, G.; Li, Y.; Qian, X.; Liu, H.; Lin, H.; Chen, N.; Li, Y. *J. Phys. Chem. C* **2011**, *115*, 2611–2615.
(19) Zhou, J.; Lv, K.; Wang, Q.; Chen, X. S.; Sun, Q.; Jena, P. *J. Chem. Phys.* **2011**, *134*, 174701.
(20) Pan, L. D.; Zhang, L. Z.; Song, B. Q.; Du, S. X.; Gao, H.-J. *Appl. Phys. Lett.* **2011**, *98*, 173102.
(21) Long, M.; Tang, L.; Wang, D.; Li, Y.; Shuai, Z. *ACS Nano* **2011**, *5*, 2593–2600.
(22) Zhang, H.; Zhao, M.; He, X.; Wang, Z.; Zhang, X.; Liu, X. *J. Phys. Chem. C* **2011**, *115*, 8845–8850.
(23) Guo, G. Y.; Lin, J. C. *Phys. Rev. B* **2005**, *71*, 165402.
(24) Topsakal, M.; Cahangirov, S.; Ciraci, S. *Appl. Phys. Lett.* **2010**, *96*, 091912.
(25) Gui, G.; Li, J.; Zhong, J. *Phys. Rev. B* **2008**, *78*, 075435.
(26) Wei, N.; Xu, L.; Wang, H.-Q.; Zheng, J.-C. *Nanotechnology* **2011**, *22*, 105705.
(27) Zhang, Y.; Wen, Y.-H.; Zheng, J.-C.; Zhu, Z.-Z. *Appl. Phys. Lett.* **2009**, *94*, 113114.
(28) Blöchl, P. E. *Phys. Rev. B* **1994**, *50*, 17953–17979.
(29) Kresse, G.; Joubert, D. *Phys. Rev. B* **1999**, *59*, 1758–1775.
(30) Kresse, G.; Hafner, J. *Phys. Rev. B* **1993**, *47*, 558–561.
(31) Kresse, G.; Furthmüller, J. *Phys. Rev. B* **1996**, *54*, 11169–11186.
(32) Perdew, J. P.; Burke, K.; Ernzerhof, M. *Phys. Rev. Lett.* **1996**, *77*, 3865–3868.
(33) Heyd, J.; Scuseria, G. E.; Ernzerhof, M. *J. Chem. Phys.* **2003**, *118*, 8207–8215.
(34) Heyd, J.; Scuseria, G. E.; Ernzerhof, M. *J. Chem. Phys.* **2006**, *124*, 219906.
(35) Monkhorst, H. J.; Pack, J. D. *Phys. Rev. B* **1976**, *13*, 5188–5192.
(36) Tersoff, J. *Phys. Rev. B* **1984**, *30*, 4874–4877.
(37) Flores, F.; Tejedor, C. *J. Phys. C* **1979**, *12*, 731–749.
(38) Tersoff, J. *Phys. Rev. B* **1985**, *32*, 6968–6971.
(39) Cardona, M.; Christensen, N. E. *Phys. Rev. B* **1987**, *35*, 6182–6194.
(40) Schleife, A.; Fuchs, F.; Rödl, C.; Furthmüller, J.; Bechstedt, F. *Appl. Phys. Lett.* **2009**, *94*, 012104.
(41) Lee, C.; Wei, X.; Kysar, J. W.; Hone, J. *Science* **2008**, *321*, 385–388.
(42) Deák, P.; Aradi, B.; Frauenheim, T.; Janzén, E.; Gali, A. *Phys. Rev. B* **2010**, *81*, 153203.
(43) Clark, C. D.; Dean, P. J.; Harris, P. V. *Proc. R. Soc. London* **1964**, *A277*, 312–329.